Graphene oxide coating facilitates the bioactivity of scaffold material for tissue engineering

Erika NISHIDA[1], Hirofumi MIYAJI[1*], Hiroko TAKITA[2], Izumi KANAYAMA[1], Maiko TSUJI[3], Tsukasa AKASAKA[4], Tsutomu SUGAYA[1], Ryuji SAKAGAMI[5], and Masamitsu KAWANAMI[1].

Affiliation

1. Department of Periodontology and Endodontology, Graduate School of Dental Medicine, Hokkaido University, Sapporo, 060-8586, Japan.
2. Support Section for Education and Research, Graduate School of Dental Medicine, Hokkaido University, Sapporo, 060-8586, Japan.
3. Mitsubishi Gas Chemical Co. Inc, Tokyo, 125-8601, Japan.
4. Department of Biomedical, Dental Materials and Engineering, Graduate School of Dental Medicine, Hokkaido University, Sapporo, 060-8586, Japan.
5. Section of Periodontology, Department of Odontology, Fukuoka Dental College, Fukuoka, 814-0193, Japan.

Abstract

Carbon-based nanomaterials are being investigated for biomedical applications. Graphene oxide (GO), a monolayer of carbon, holds promise as a tissue engineering substrate due to its unique physicochemical properties. The aim of this study was to evaluate the effect of a GO coating on cell proliferation and differentiation in vitro. We also assessed the bioactivities of collagen scaffolds coated with different concentrations of GO in rats. The results showed that GO affects both cell proliferation and differentiation, and improves the properties of collagen scaffolds. Subcutaneous implant tests showed that low concentrations of GO scaffold enhances cell in-growth and is highly biodegradable, whereas high concentrations of GO coating resulted in adverse biological effects. Consequently, scaffolds modified with a suitable concentration of GO are useful as a bioactive material for tissue engineering.

1. Introduction

Carbon-based nanomaterials hold promise for biomedical applications. Nanocarbon materials, such as carbon nanotubes (CNTs) [1-3], carbon nanohorns [4], carbon nanofibers [5], fullerene [6], and graphene [7], have been extensively studied in recent years. It has been reported that graphene oxide (GO), a monolayer of carbon, is a good tissue engineering substrate due to its unique physicochemical properties, including large surface area, high dispersibility and hydrophilicity [8]. GO can promote biological interactions due to its many surface functional groups [9, 10]. Several investigators have reported that GO can serve as a carrier for drugs and other biomolecules [11, 12]. In addition, GO regulates the proliferation and differentiation of cultured mesenchymal stem cells [13-15]. GO will likely be used in combination with other materials [16-18] or growth factors [19, 20] in future medical applications, playing a facilitative role with other tissue engineering materials.

Regenerative medicine is the process of tissue engineering of previously irreparable tissues or organs. Tissue engineering strategies involve three major elements: cells, signaling molecules, and natural or artificial scaffolds. Such scaffolds have been developed for use in various tissues such as bone [21-23], cartilage [23], muscle, [24] and skin [25]. Scaffolds for use in regenerative medicine provide the base for the repopulation and specialization of stem cells, blood vessels and extracellular matrices [26]. In general, the surface morphology of the scaffold strongly affects the attachment of surrounding cells and tissues after implantation [27]. Recently, nano-sized substances have been investigated for use as biomaterials [28, 29]. Nanostructures at the surface of the base material enhance some bioactivities due to quantum size effects and the material's large surface area [30, 31]. Early contact between regenerative cells or tissues and the nanostructures facilitate the tissue-reforming process. Previous studies reported that collagen sponge coated with nano-sized particles of ceramics exhibited cell and tissue ingrowth, bone formation, and high biodegradation [32, 33]. Therefore, we hypothesized that nanomodification using GO would provide novel properties to the scaffold and up-regulate the tissue-reforming process. Although we previously developed GO-coated collagen scaffolds, the effects of the GO coating have not yet been investigated in vivo. Accordingly, the aim of this study was to evaluate the bioactivities of collagen scaffolds coated with different concentration of GO in rats to assess the biocompatibility and biodegradability of the scaffolds. We also evaluated the effects of GO coating on cell proliferation and differentiation in vitro.

2. Materials and methods

2.1 Preparation of GO coating film

Aqueous GO dispersion (1 wt%, Mitsubishi Gas Chemical, nano GRAX®) was prepared as described previously [34]. The thickness of the GO monolayer was ~1 nm and the average width was about 20 μm. Thin GO films were prepared on culture plates (40 mm dish, Trasadingen, TPP) using 1 ml of 0.1 or 1 wt% of GO [Figs. 1(a) and (b)]. The hydrophilicity of the films was investigated using a contact angle meter (Kyowa Electronic Instruments, DMs-200).

2.2 Cell morphology

1×10^4 mouse osteoblastic MC3T3-E1 cells (RIKEN Bioresource Center) were seeded on each GO film and cultured in humidified 5% CO_2 at 37°C using medium (Life Technologies, MEM alpha-GlutaMAX-I) supplemented with 10% fetal bovine serum (FBS; Life Technologies, Qualified) and 1% antibiotics (Life Technologies, Pen Strep). A culture plate without GO coating was used as a control. After 24 h of culture, samples were fixed in 2.5% glutaraldehyde in 0.1 M sodium cacodylate buffer (pH 7.4) for 30 min and rinsed in cacodylate buffer solution. Films were then dehydrated in increasing concentrations of ethanol. Following critical point drying, samples were analyzed using a scanning electron microscope (SEM; Hitachi, S-4000) at an accelerating voltage of 10 kV after coating with a thin layer of Pt-Pd.

2.3 Measurement of DNA content and ALP activity

The DNA content and alkaline phosphatase (ALP) activity of cells attached to the GO film was measured. 1×10^4 mouse osteoblastic MC3T3-E1 cells were seeded on each film and cultured for 7, 14, 21, or 28 days in humidified 5% CO_2 at 37°C using medium supplemented with 10% FBS and 1% antibiotics. A culture plate without GO was used as a control. The incubated specimens were rinsed twice using phosphate buffered saline (PBS), then the cells were lysed using 0.5 ml PBS with subsequent sonication for 10 s. 50 µl of the cell suspension was added to 50 µl of 4 M NaCl, 0.1 M phosphate buffer (pH 7.4). After centrifugation, DNA content was measured using a DNA quantification kit (Primary Cell) according to the manufacturer's instructions. DNA was measured using a fluorescence spectrophotometer (Hitachi, F-3000) equipped with a 356 nm excitation filter and 458 nm emission filter. ALP activity was assayed after 14 or 28 days' cell culture by adding 50 µl of cell suspension to 50 µl of 0.4% IGEPAL, 20 mM Tris-HCl, 2 mM $MgCl_2$, pH 7.4. After centrifugation, ALP activity was measured using a LabAssay ALP kit (Wako). Optical density was measured on a microplate reader (Toyo Sokki, ETY-300) using an absorbance of 405 nm. ALP activity was normalized by DNA content.

2.4 Fabrication and characterization of GO-coated collagen scaffold

GO at different concentrations (0.01, 0.1, and 0.5 wt%) in 1-methyl-2-pyrrolidinone solution was prepared for coating collagen scaffolds. One hundred microliters of GO-solution was injected into each collagen scaffold ($6 \times 6 \times 3$ mm^3, an average porosity of 97.3%, Olympus Terumo Biomaterials, Terudermis). Then the scaffolds were rinsed with ethanol and air-dried [Fig. 4(a)]. Scaffold without GO coating was used as a control. The porosity of the scaffolds was calculated according to the following equation: porosity = $100 \times (1-\rho_1/\rho_2)$, where ρ_1 is the bulk density, ρ_2 is the theoretical density of the scaffold. Subsequently, GO-coated scaffold was characterized by SEM observation and compression tests. The compressive strength was measured using a universal testing machine (Shimadzu, EZ-S) with the cross-head loading speed set at 0.5 mm/min.

2.5 Biocompatible test for GO-coated scaffold

In order to evaluate cytocompatibility, 4×10^4 MC3T3-E1 cells were seeded on GO-coated scaffold and cultured in humidified 5% CO_2 at 37° C using medium supplemented with 10% FBS and 1% antibiotics. Cell viability was assessed after 1, 3, and 7 days' culture using a cell counting kit-8 (Dojindo Laboratories, CCK-8) following the manufacturer's instructions. Optical density was measured using a microplate reader at an absorbance of 450 nm. Some samples were fixed in 2.5% glutaraldehyde in 0.1 M sodium cacodylate buffer (pH 7.4) for 30 min and rinsed in cacodylate buffer solution. Scaffolds were then dehydrated in increasing concentrations of ethanol and analyzed by SEM.

2.6 Surgical procedure

The experimental protocol followed the institutional animal use and care regulations of Hokkaido University [35]. Eighteen 10-week-old male Wistar rats weighing 190 to 210 g were given general anesthesia by intraperitoneal injection of 0.6 ml/kg sodium pentobarbital (Kyoritsu Seiyaku, Somnopenthyl), as well as a local injection of 2% lidocaine hydrochloride with 1:80,000 epinephrine (Dentsply-Sankin, Xylocaine Cartridge for Dental Use). After a skin incision was made, each scaffold was implanted into the subcutaneous tissue of the back of each rat. Skin flaps were sutured (GC, Softretch 4-0) and tetracycline hydrochloride ointment (POLA Pharma, Achromycin Ointment) was applied to the wound. Rats were euthanized using an overdose of sodium pentobarbital (2 ml/kg) at 10 or 35 days post-surgery.

2.7 DNA content of implanted scaffolds

Several implants were extracted from the wound after 10 days and freeze-dried. Following pulverization, the DNA content of each sample was examined using a DNA quantification kit.

2.8 Histological analysis

Several samples at 10 and 35 days were collected for histological observation. The tissue blocks, including the surrounding soft tissue, were fixed in 10% buffered formalin, embedded in paraffin wax, and cut into 6 μm sections. Sections were stained with hematoxylin-eosin (HE). Three stained sections were taken, one from the center of the scaffold and one 1 mm from either side of the center, and examined the sections using light microscopy. Histomorphometric measurements, including the area of the implanted scaffold, tissue ingrowth, and the number of giant cells, were performed using a software package (National Institute of Health, Image J 1.41).

2.9 Statistical analysis

The means and standard deviations of each parameter were calculated for each group. Statistical analysis was performed using the Scheffé test on each measurement. P-values <0.05 were considered statistically significant. All statistical procedures were performed using a software package (SPSS

Japan, DR. SPSS 11.0).

3. Results

3.1 In vitro assessment of GO film

Contact angle measurements revealed the highly hydrophilic nature of GO. The contact angle to 1 wt% GO film [Fig. 1(e)] was significantly lower than that to 0.1wt% GO [Fig. 1(d)] and to the culture dish [Fig. 1(c)]. SEM observation revealed that osteoblastic MC3T3-E1 cells attached to the GO film [Fig. 2], but cell spreading was suppressed on films with a high concentration of GO compared to the culture dish control [Figs. 2(e) and 2(f)]. The time-dependent increase in DNA levels in 0.1 wt% GO was similar to that of the control, suggesting that a low concentration of GO in the film exhibits good cytocompatibility. However, films with a high concentration of GO significantly inhibited both cell proliferation and ALP activity [Fig. 3].

3.2 Characterization of GO-coated scaffold

GO nanosheets attached to the surface of collagen scaffold fibers were observed using SEM [Figs. 4(b)-4(g)]: low concentrations of GO showed a corrugated surface whereas high concentrations of GO showed a rough surface. The GO- modified surface was also confirmed on the central region of the scaffold [Fig. 4(g)]. The porosity of each scaffold was calculated to be > 96%. There was no significant difference in porosity between non-coated and 0.01 wt% GO-coated scaffold. The compressive strength of GO-coated scaffold was approximately 4-fold greater than that of the collagen-only scaffold, a difference that is statistically significant. In addition, the strength of 0.5 wt% GO-coated scaffold was significantly greater than that of 0.01 and 0.1 wt% GO-coated scaffold [Table I].

3.3 Cytocompatibility of GO-coated scaffold

Osteoblastic MC3T3-E1 cell proliferation on 0.01 wt% GO-coated scaffold was equivalent to that of the control. In contrast, cell proliferation was significantly inhibited on 0.1 and 0.5 wt% GO-coated scaffold [Fig. 5(a)]. SEM observation revealed attached, spread and elongated cells on the collagen scaffold coated with 0.01 wt% GO [Fig. 5(b)], suggesting that 0.01 wt% GO-coated scaffold exhibits good cytocompatibility.

3.4 Histological observations at 10 days

Limited cell and tissue in-growth was observed in the implanted control collagen scaffold material, with the interior of the control scaffold considerably compressed and incompatible with supporting cell invasion and tissue formation. Inflammatory responses were rarely observed around the implants [Figs. 6(a)-6(c)]. GO-coated scaffolds resulted in various bioactivities in rats. For example, regenerative space was maintained by GO coating [Figs. 6(d), 6(g), and 6(j)]. In 0.01 wt% GO-coated scaffolds, ingrowth of fibroblastic cells and blood vessels was frequently observed [Figs.

6(e)-6(f)]. Inflammatory cells, including leukocytes and lymphocyte, were rarely seen around each material, regardless of the GO concentration, indicating that the GO-modified material exhibits good biocompatibility. However, numerous giant cells associated with the resorption of materials appeared at the periphery of 0.1 and 0.5 wt% GO-coated scaffolds [Figs. 6(h) and 6(k)], and little cell penetration was observed in the centers of these scaffolds [Figs. 6(i) and 6(l)].

3.5 Histological observations at 35 days

In the control group, considerable resorption of the implant was clearly detectable [Fig. 7(a)]. Evidence of cell ingrowth with giant cells was frequently observed in the residual scaffold material [Fig. 7(b)]. Modification with 0.01 wt% GO stimulated bioactivities associated with material degradation, and most of the collagen scaffold had disappeared, similar to the control [Fig. 7(c)]. Tissue ingrowth was frequently demonstrated in the scaffold [Fig. 7(d)]. In contrast, histological specimens of 0.1 or 0.5 wt% GO-coated collagen scaffolds exhibited evidence of residual scaffold material [Figs. 7(e) and 7(g)]. These GO-coated scaffolds were engulfed by macrophage-like giant cells [Fig. 7(f)]. Little cell infiltration was observed in the center of the residual scaffold material, suggesting that little tissue replacement by remodeling had occurred. In addition, residual GO films were frequently observed at the periphery of 0.5 wt% GO-coated scaffolds [Fig. 7(h)].

3.6 Histomorphometric analysis

The degree of cell ingrowth, DNA content and number of giant cells after implantation of each material are presented in Figs. 8(a)-8(c). Cell ingrowth of 0.01 wt% GO-coated scaffold was significantly greater than of other scaffolds, whereas both DNA content and giant cell numbers increased in a GO dose-dependent manner. A high concentration GO groups is apparently associated with the accumulation of macrophage-like cells.

Measurements of the degradability of each scaffold are presented in Figure 8D. Both 0.01 wt% GO scaffold and the control degraded rapidly, whereas there was significant residual scaffold from the 0.5 wt% GO scaffold at 10 and 35 days.

4. Discussion

Regenerative scaffolds need to exhibit biologically compatible surface morphology, porosity, physical strength and biocompatibility [36]. In the present study, SEM observations revealed clear morphological changes of collagen scaffolds following GO-coating. Ordinarily, the cell-biomaterial interfacial morphology strongly affects the induction of cell reactions [37, 38]. Many investigators have demonstrated that nano-/micro scale structures of bio-based materials exhibit advantageous properties for tissue engineering processes [39-41]. Additionally, nano-modification can increase the surface area of biomaterials for cell attachment and signaling molecules adsorption [42]. Therefore, nano-modifications using GO might provide good structure for colonization by several cell types and multi-cellular organisms.

In general, the physical strength of the regenerative scaffold plays a facilitative role in maintaining space for cell ingrowth [22, 43]. In this study, GO coating significantly raised the compressive strength of the collagen scaffolds, likely due to the GO nanosheet assembling on the strut of the collagen scaffold and reinforcing the scaffold. Regenerative scaffolds are designed to have high porosity for tissue ingrowth, but a highly porous structure lowers physical strength [44]. SEM images showed that collagen sponge foam coated with GO had porous, open interior spaces required for cell colonization. Furthermore, the high porosity of GO scaffolds was confirmed by calculations of the porous structure. Taken together, the data indicate that GO coating reinforces collagen sponge stability without altering its porous structure.

Inflammatory cells such as neutrophils and lymphocytes were rarely seen around the GO-modified implants, and fibroblast cells and blood vessels frequently penetrated scaffolds coated with 0.01 wt% GO. Collagen scaffolds consisting of atelocollagen are a biocompatible material [45, 46]. Our results indicate that collagen scaffold coated with a low concentration of GO is a good biocompatible material. However, histological specimens in contact with scaffolds with high concentrations of GO showed the accumulation of macrophage-like giant cells, whereas no significant increase in DNA content and or cell proliferation was observed in vitro. These biological responses may be caused by an overdose of GO, so optimum concentrations of GO should be used to prevent reactions detrimental to healing. We speculate that inhibitory biological effects are involved in a high concentration of GO. Cells attach to hydrophobic surfaces via their cell membrane [47, 48], but 1 wt% GO films provide a fairly hydrophilic surface. Lee et al. have demonstrated that contact angle of GO film was lower than that of reduced GO film without functional groups [14]. Therefore, many hydrophilic groups would cause low cell adhesion on a high concentration GO coating. In addition, GO induced significant production of reactive oxygen species (ROS) which slightly decreases cell viability [49]. It therefore seems likely that ROS production and a hydrophilic surface resulting from a high concentration GO coating increase cytotoxity and suppress cell proliferation both in vitro and in vivo.

Regenerative scaffolds must support the rapid growth of reforming tissue at the healing site. Histological measurements showed that 0.01 wt% GO-coated scaffold resorbed easily into reconstructed tissue. In contrast, 0.5 wt% GO-coated scaffold was scarcely phagocytized, regardless of the accumulation of macrophage-like cells. Therefore, it was suggested that scaffold coated with a high concentration of GO exhibited low degradation in the body. In general, infection risk is increased by residual material exposure. Furthermore, previous histological findings indicated that GO was frequently engulfed by macrophage-like cells, and there was evidence of residual graphene in cell lysosomes following phagocytosis [50]. In contrast, long-term (2 year) histological examination revealed that oxidized CNTs had degraded inside macrophages in rat subcutaneous tissue [51]. The degradation of GO-based nanomaterials, and a systematic method for testing the safety of nanocarbon materials, must be established in the future.

5. Conclusions

The present study focused on the effects of a graphene oxide coating on the cell proliferation and differentiation of biomaterials for developing a tissue engineering scaffold. GO coating improved several biomedical properties of collagen scaffold including surface structure, compressive strength and cell ingrowth. A low concentration GO film did not inhibit cell proliferation or differentiation in vitro, and enhanced biocompatibility and biodegradability. Therefore, scaffold modified by a suitable concentration of GO holds promise as a biomaterial for tissue engineering.

Acknowledgments

We thank Olympus Terumo Biomaterials Corporation. for providing the collagen scaffold. This work was supported by JPSP KAKENHI Grant Number 25463210. The authors report no conflicts of interest related to this study.

References

1) P. A. Tran, L. Zhang and T. J. Webster: Adv. Drug Delivery. Rev. **61** (2010) 667.

2) Y. Usui, K. Aoki, N. Narita, N. Murakami, I. Nakamura, K. Nakamura, N. Ishigaki, H. Yamazaki, H. Horiuchi, H. Kato, S. Taruta, Y. A. Kim, M. Endo and N. Saito: Small **4** (2008) 240.

3) Z. J. Han, A. E. Rider, M. Ishaq, S. Kumar, A. Kondyurin, Marcela M. M. Bilek, I. Levchenko and K. Ostrikov: RSC Adv. **3** (2013) 11058.

4) T. Kasai, S. Matsumura, T. Iizuka, K. Shiba, T. Kanamori, M. Yudasaka, S. Iijima and A. Yokoyama: Nanotechnology **22** (2011) 065102.

5) K. L. Elias, R. L. Price and T. J. Webster: Biomaterials **23** (2002) 3279.

6) R. Partha and J. L. Conyers: Int. J. Nanomed. **4** (2009) 261.

7) O. N. Ruiz, K. A. S. Fernando, B. Wang, N. A. Brown, P. G. Luo, N. D. McNamara, M. Vangsness, Y. Sun and C. E. Bunker: ACS Nano **5** (2011) 8100.

8) D. R. Dreyer, S. Park, C. W. Bielawski and R. S. Ruoff: Chem. Soc. Rev. **39** (2010) 228.

9) Y. Zhu, S. Murali, W. Cai, X. Li, J. W. Suk, J. R. Potts and R. S. Ruoff: Adv. Mater. **22** (2010) 3906.

10) M. Tang, Q. Song, N. Li, Z. Jiang, R. Huang and G. Cheng: Biomaterials **34** (2013) 6402.

11) J. Hong, N. J. Shah, A. C. Drake, P. C. DeMuth, J. B. Lee, J. Chen and P. T. Hammond: ACS Nano **6** (2012) 81.

12) L. Zhang, J. Xia, Q. Zhao, L. Liu and Z. Zhang: Small **6** (2010) 537.

13) G. -Y. Chen, D. W. -P. Pang, S. -M. Hwang, H. -Y. Tuan and Y. -C. Hu: Biomaterials **33** (2012) 418.

14) W. C. Lee, C. H. Y. X. Lim, H. Shi, L. A. L. Tang, Y. Wang, C. T. Lim and K. P. Loh: ACS Nano **5** (2011) 7334.

15) T. R. Nayak, H. Andersen, V. S. Makam, C. Khaw, S. Bae, X. Xu, P. R. Ee, J. Ahn, B. H. Hong,

G. Pastorin and B. Ozyilmaz: ACS Nano **5** (2011) 4670.

16) H. Bao, Y. Pan, Y. Ping, N. G. Sahoo, T. Wu, L. Li, J. Li and L. H. Gan: Small **7** (2011) 1569.

17) X. Sun, Z. Liu, K. Welsher, J. T. Robinson, A. Goodwin, S. Zaric and H. Dai: Nano Res. **1** (2008) 203.

18) K. Yang, J. Wan, S. Zhang, Y. Zhang, S. Lee and Z. Liu: ACS Nano **5** (2011) 516.

19) W. La, S. Park, H. Yoon, G. Jeong, T. Lee, S. H. Bhang, J. Y. Han, K. Char and B. Kim: Small. **9** (2013) 1.

20) X. Shi, H. Chang, S. Chen, C. Lai, A. Khademhosseini and H. Wu: Adv. Mater. **22** (2011) 751.

21) H. Miyaji, T. Sugaya, K. Ibe, R. Ishizuka, K. Tokunaga and M. Kawanami: J. Periodont. Res. **45** (2010) 658.

22) S. Shimoji, H. Miyaji, T. Sugaya, H. Tsuji, T. Hongo, M. Nakatsuka, K. U. Zaman and M. Kawanami: J. Periodont. **80** (2009) 505.

23) D. W. Hutmacher: Biomaterials **21** (2000) 2529.

24) K. D. McKeon-Fischer, D. H. Flagg and J. W. Freeman: J. Biomed. Mater. Res. A 99 (2011) 493.

25) L. Ma, C. Gao, Z. Mao, J. Zhou, J. Shen, X. Hu and C. Han: Biomaterials **24** (2003) 2529.

26) F. Chen and Y. Jin: Tissue Eng, Part B. **16** (2010) 219.

27) D. E. Ingber: *Principles of Tissue Engineering* (Elsevier Academic Press, Burlington, 2000) p.101.

28) B. Ji and H. Gao: J. Mech. Phys. Solids **52** (2004) 1963.

29) F. Watari, N. Takashi, A. Yokoyama, M. Uo, T. Akasaka, Y. Sato, S. Abe, Y. Totsuka and K. Tohji: J. R. Soc. Interface **6** (2009) 371.

30) A. E. Nel, L. Mädler, D. Velegol, T. Xia, E. M. V. Hoek, P. Somasundaran, F. Klaessig, V. Castranova and M. Thompson: Nat. Mater. **8** (2009) 543.

31) E. Engel, A. Michiardi, M. Navarro, D. Lacroix and J. A. Planell: Trends in Biotechnology **26** (2008) 39.

32) S. J. Kalita, A. Bhardwaj and H. A. Bhatt: Mater. Sci. Eng. C **27** (2007) 441.

33) A. Ibara, H. Miyaji, B. Fugetsu, E. Nishida, H. Takita, S. Tanaka, T. Sugaya and M. Kawanami: J. Nanomater. **2013** (2013) 639502.

34) M. Hirata, T. Gotou, S. Horiuchi, M. Fujiwara and M. Ohba: Carbon **42** (2004) 2929.

35) Animal Research Committee of Hokkaido University, Approval No. 13-76.

36) A. J. Salgado, O. P. Coutinho and R. L. Reis: Macromol. Biosci. **4** (2004) 743.

37) M.J. Dalby, M.O. Riehle, H. Johnstone, S. Affrossman and A.S.G. Curtis: Biomaterials **23** (2002) 2945.

38) P. Ducheyne and Q. Qiu: Biomaterials **20** (1999) 2287.

39) K. Anselme: Biomaterials **21** (2000) 667.

40) L.A. Smith and P.X. M: Biomaterials **39** (2004) 125.

41) K. Tuzlakoglu, N. Bolgen, A. J. Salgado, M. E. Gomes, E. Piskin and R. L. Reis: J. Mater. Sci. Mater. Med. **16** (2005) 1099.

42) F. Yang, R. Murugan, S. Ramakrishna, X. Wang, Y. –X. Ma and S. Wang: Biomaterials **25** (2004) 1891.

43) X. Liu, L. A. Smith, J. Hu and P. X. Ma: Biomaterials **30** (2009) 2252.

44) V. Karageorgiou and D. Kaplan: Biomaterials **26** (2005) 5474.

45) J. Glowacki and S. Mizuno: Biopolymers **89** (2008) 125.

46) Y. Kosen, H. Miyaji, A. Kato, T. Sugaya and M. Kawanami: J. Periodont. Res. **47** (2012) 626.

47) A. Kushida, M. Yamato, C. Konno, A. Kikuchi, Y. Sakurai and T. Okano: J. Biomed. Mater. Res. A **51** (2000) 216.

48) B. R. McAuslan and G. Johnson: J. Biomed. Mater. Res. **21** (1987) 921.

49) Y. Chang, S. Yang, J. Liu, E. Dong, Y. Wang, A. Cao, Y. Liu and H. Wang: Toxicol. Lett. **200** (2011) 201.

50) K. Wang, J. Ruan, H. Song, J. Zhang, Y. Wo, S. Guo and D. Cui: Nanoscale Res. Lett. **6** (2011)

51) Y. Sato, A. Yokoyama, Y. Nodasaka, T. Kohgo, K. Motomiya, H. Matsumoto, E. Nakazawa, T. Numata, M. Zhang, M. Yudasaka, H. Hara, R. Araki, O. Tsukamoto, H. Saito, T. Kamino, F. Watari and K. Tohji: Sci. Rep. **3** (2013) 2516.

Table I. Structural parameters of each scaffold (N = 6, mean ± SD)

	Control	0.01 wt% GO	0.1 wt% GO	0.5 wt% GO
Weight (mg/mm^3)	0.038 ± 0.002	0.041 ± 0.005	0.049 ± 0.004*	0.128 ± 0.020*
Porosity (%)	97.30 ± 0.17	97.17 ± 0.29	96.87 ± 0.29*	96.73 ± 0.09*
Compressive strength (Mpa)	0.073 ± 0.007	0.131 ± 0.019^a	0.152 ± 0.018*	0.352 ± 0.100$^{*, \dagger}$

*: P<0.05, vs, control and †: P<0.05, vs, 0.01 and 0.1 wt% GO scaffold.

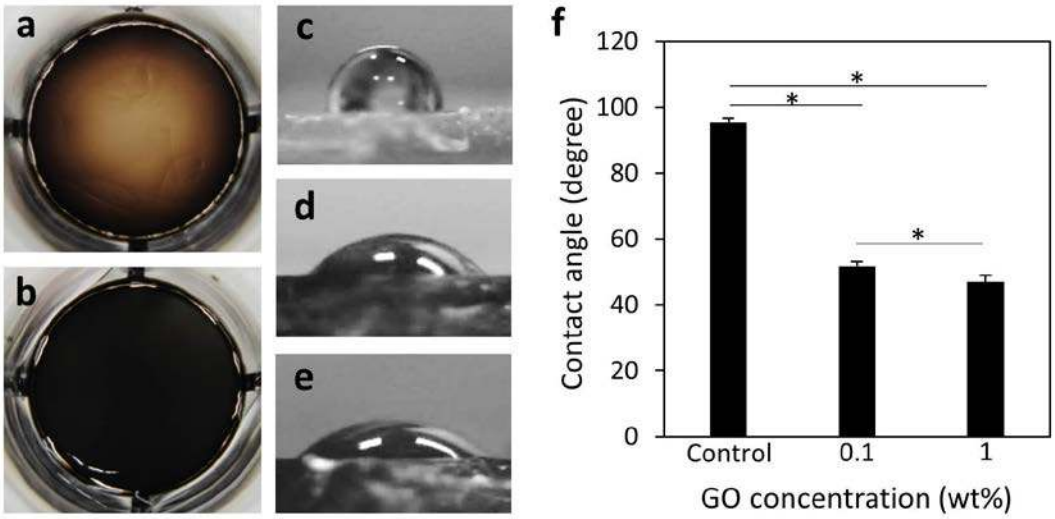

Fig.1 GO films using 0.1 wt% GO (a) and 1 wt% GO (b). Contact angle image of a culture dish, used as a control (c), 0.1 wt% GO film (d) and 1 wt% GO film (e). (f) Summary of the contact angle (N = 5, mean ± SD). *P < 0.05

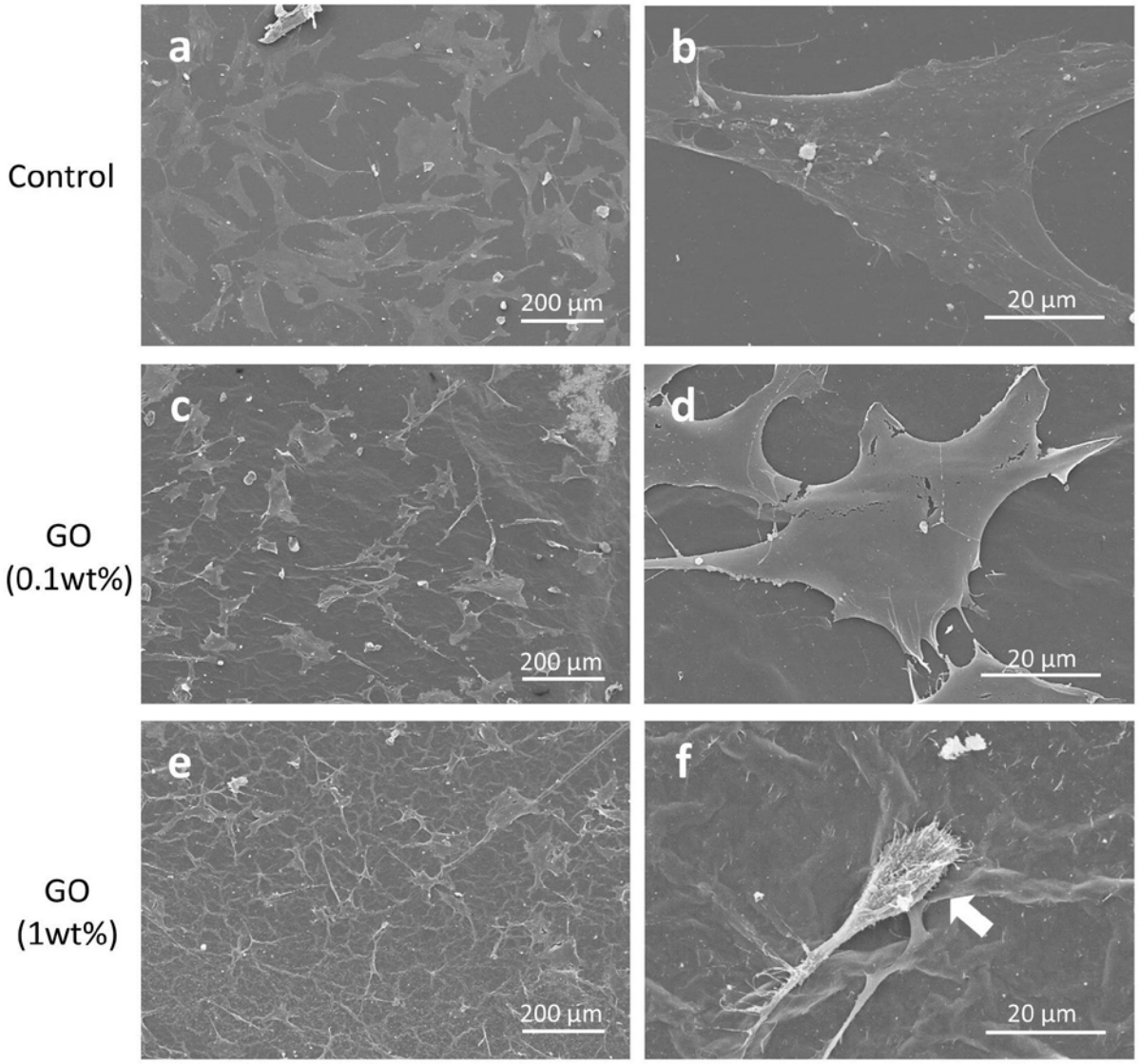

Fig.2 SEM micrograph of cell morphology. (a, b) Control (culture dish). (c, d) 0.1 wt% GO film. (e, f) 1 wt% GO film. Cell spreading was suppressed on 1 wt% GO film (white arrow).

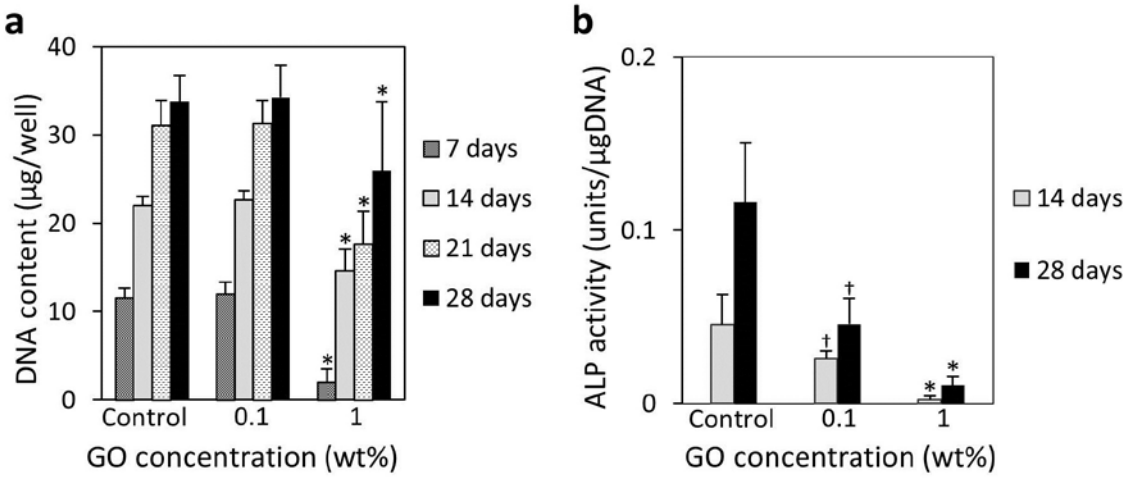

Fig.3 In vitro assessment of each film (N = 8, mean ± SD). (a) DNA content. (b) ALP activity. *: P<0.05, vs, control and 0.1 wt% GO film. †: P<0.05, vs, control.

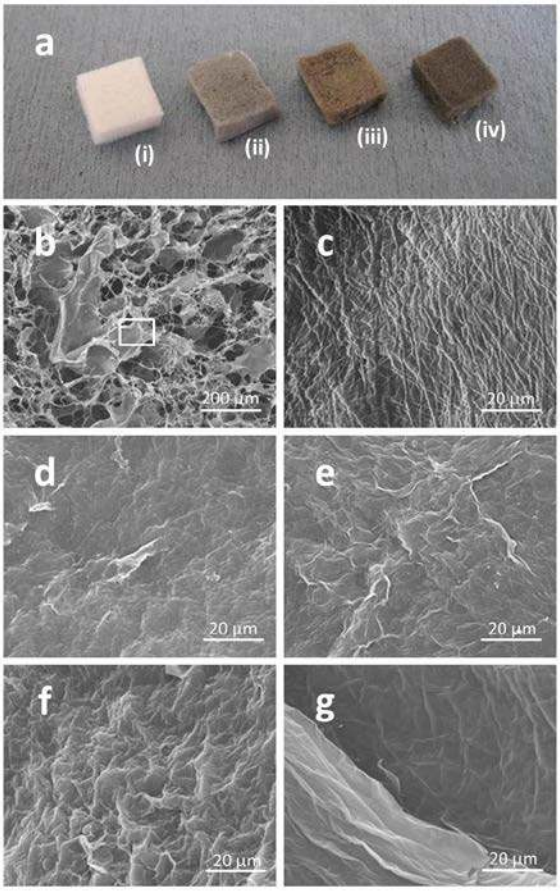

Fig.4 (a) collagen scaffold (i) and collagen scaffold coated with 0.01 wt% GO (ii), 0.1 wt% GO (iii) and 0.5 wt% GO (iv). (b) SEM micrograph of the collagen scaffold. (c) Higher magnification of the collagen scaffold. (d) Higher magnification of 0.01 wt% GO scaffold. (e) Higher magnification of 0.1 wt% GO scaffold. (f) Higher magnification of 0.5 wt% GO scaffold. (g) The inner surface of the 0.5 wt% GO scaffold. The nanomodified surface is evident.

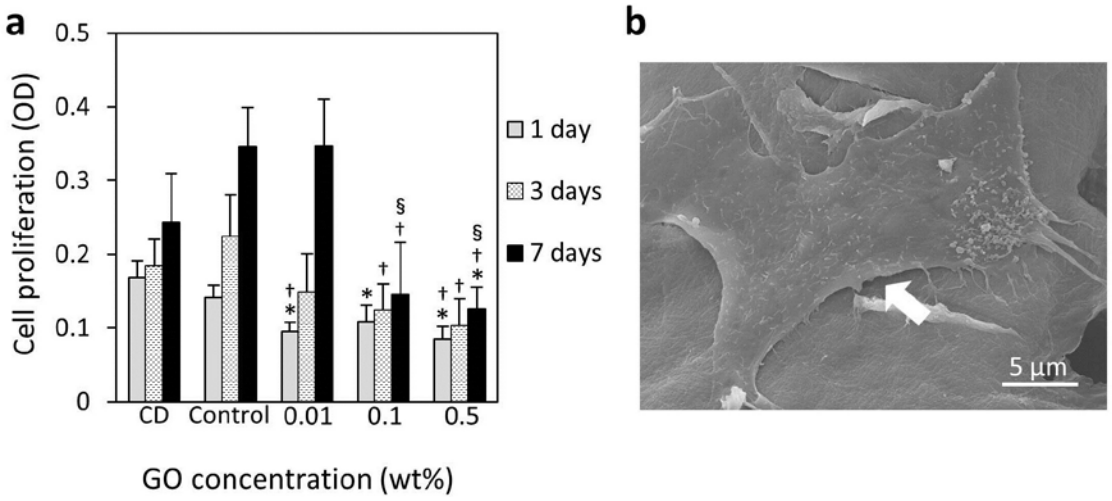

Fig.5 (a) CCK-8 assays of MC3T3-E1 cell proliferation after 1, 3, and 7 days incubation (N = 6, mean ± SD). CD, ctrl, indicate culture dish and control, respectively. *: P<0.05, vs, culture dish, †: P<0.05, vs, control and §: P<0.05, vs, 0.01 wt % GO coated scaffold. (b) SEM images of collagen scaffold coated with 0.01 wt% GO. Cell spreading on the scaffolds is shown (white arrows).

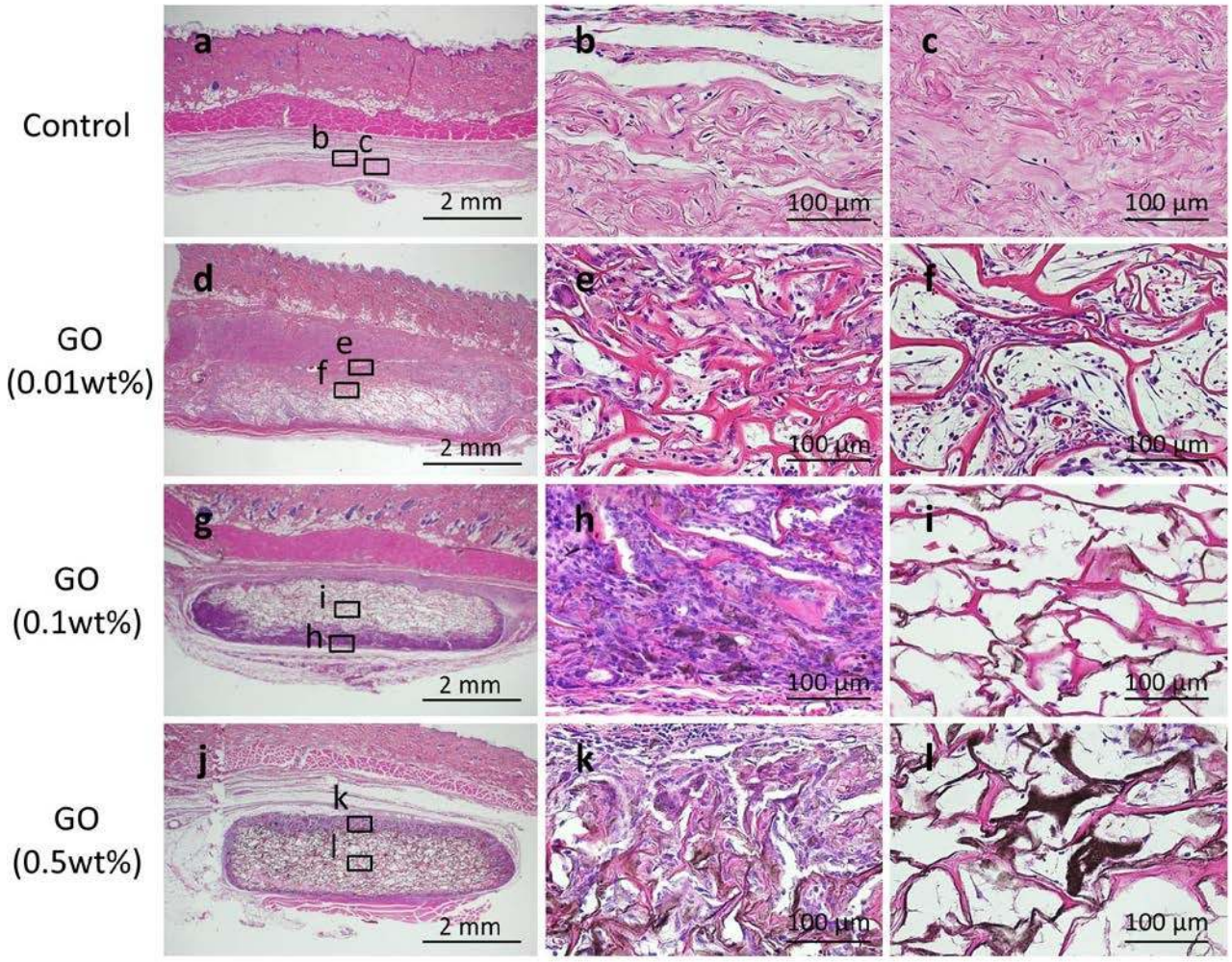

Fig.6 Histological findings at 10 days. (a) Specimen following implantation of collagen scaffold. (b, c) Higher magnification of the framed area in (b, c). Sponge form was compressed and little cell and tissue ingrowth were observed in the collagen scaffold. (d) Specimen following implantation of 0.01 wt% GO-coated scaffold. (e, f). Higher magnification of the framed area in (e, f). Ingrowth of fibroblastic cells and blood vessels was frequently observed. (g) Specimen following implantation of 0.1 wt% GO-coated scaffold. (h, i) Higher magnification of the framed area in (h, i). Tissue ingrowth was limited at the periphery of the scaffold. (j) Specimen following implantation of 0.5 wt% GO-coated scaffold. (k, l) Higher magnification of the framed area in (k, l). Giant cells (arrows) were found at the periphery of the scaffold. Little cell penetration was observed at the central region. HE staining.

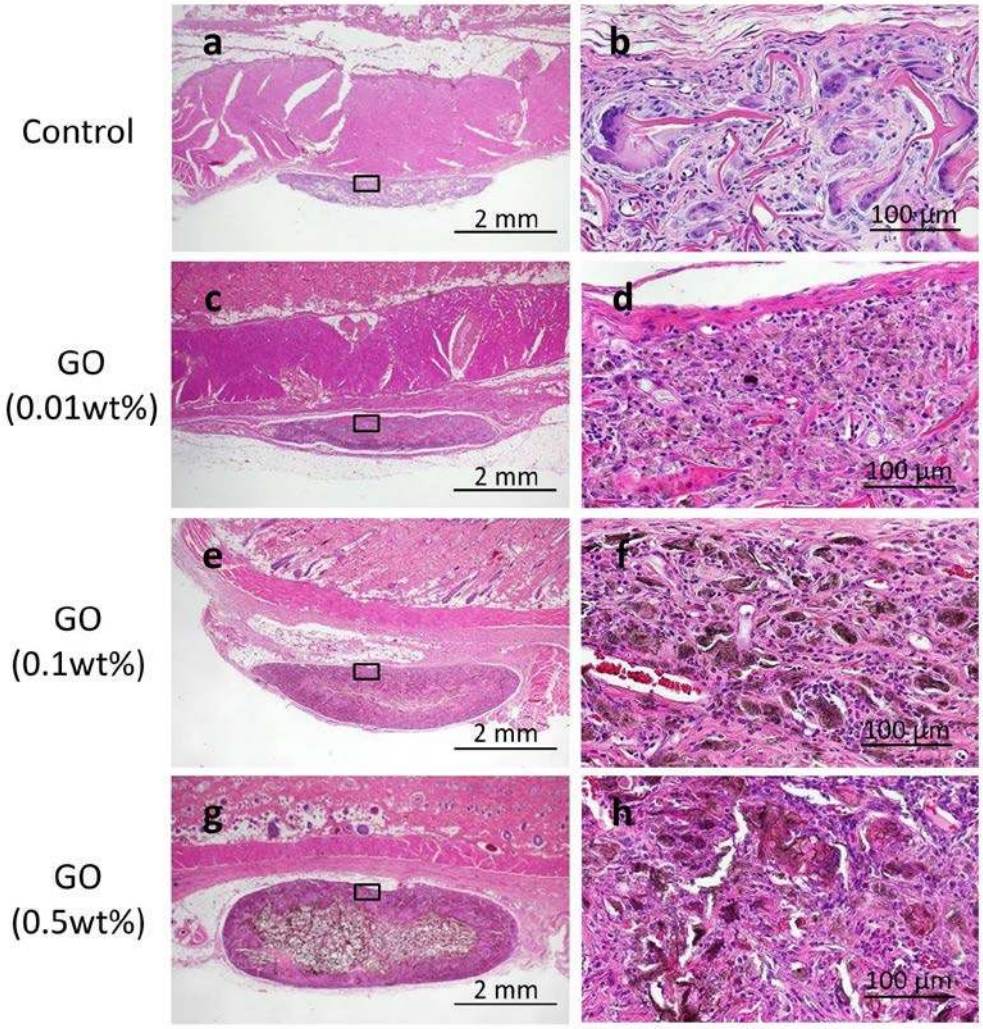

Fig.7 Histological findings at 35 days. (a) Specimen following implantation of collagen scaffold. (b) Higher magnification of the framed area in (a). Collagen scaffold has largely degraded. (c) Specimen following implantation of 0.01 wt% GO-coated scaffold. (d) Higher magnification of the framed area in (c). Tissue ingrowth was frequently demonstrated in the 0.01 wt% GO-coated scaffold. (e) Specimen following implantation of 0.1 wt% GO-coated scaffold application. (f) Higher magnification of the framed area in (e). (g) Specimen following implantation of 0.5 wt% GO-coated scaffold application. (h) Higher magnification of the framed area in (g). 0.1 and 0.5 wt% GO-coated scaffold exhibited evidence of residual material. HE staining.

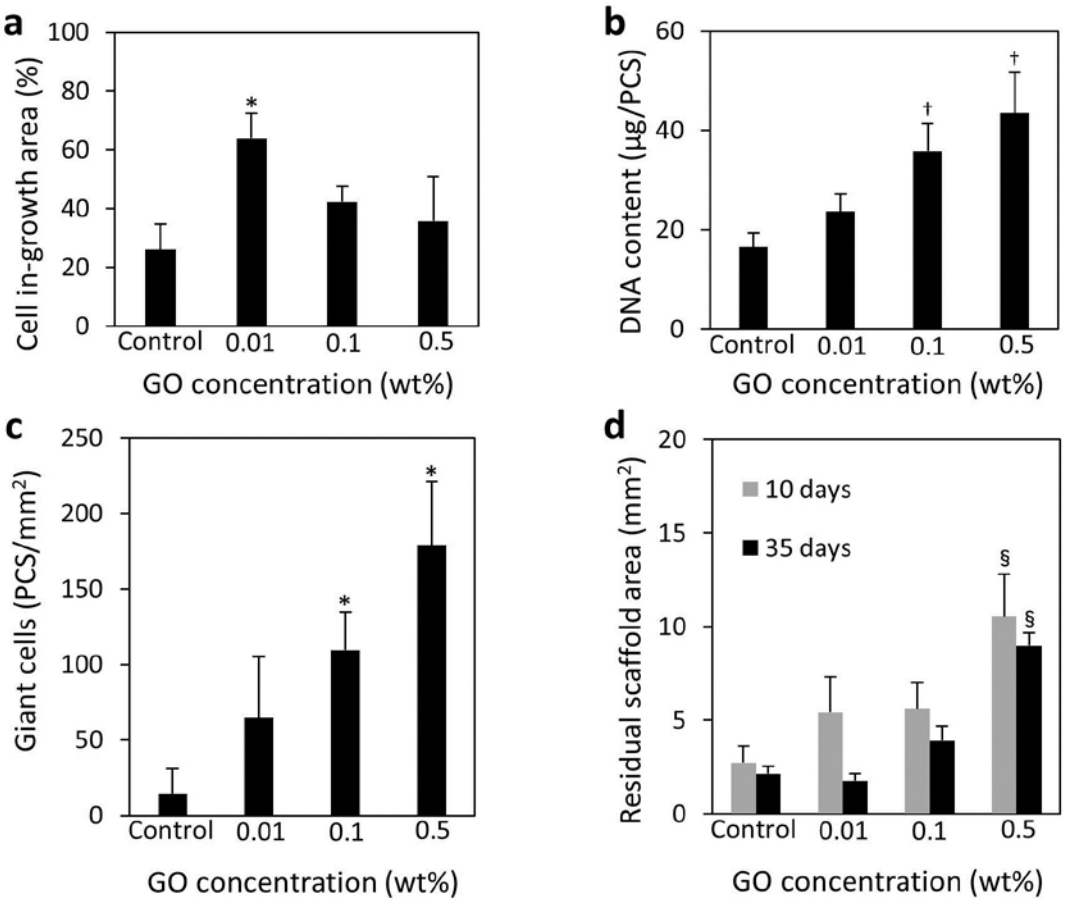

Fig.8 In vivo assessment (N = 6, mean ± SD). (a) Cell in-growth area at 10 days. (b) DNA content of implanted scaffold at 10 days. (c) Number of giant cells at 10 days. (d) Residual scaffold area at 10 and 35 days. *: $p<0.05$, vs, control. †: $P<0.05$, vs, control and 0.01 wt% GO scaffold. §: $P<0.05$, vs, control, 0.01, and 0.1 wt% GO scaffold.